Reduction of short chain alkynes by a nitrogenase α-70^Ala-substituted MoFe protein †

Suzanne M. Mayer,* Walter G. Niehaus and Dennis R. Dean

Department of Biochemistry-Fralin Biotechnology Center, Virginia Tech, Blacksburg, Virginia, 24061, USA. E-mail: sumayer@vt.edu

The Mo-dependent nitrogenase comprises two component proteins, called the Fe protein and MoFe protein, which together catalyze the nucleotide-dependent reduction of N_2 to NH_3. Nitrogenase also catalyzes the reduction of a variety of other multiply bonded substrates including the short chain alkyne acetylene. Substrate reduction is known to occur at an Fe_7S_9Mo : homocitrate cluster, designated FeMo-cofactor. Despite 40 years of intensive research and knowledge of the macromolecular structures of the nitrogenase component proteins from several different sources, the mechanism for the binding, activation and reduction of N_2 is still unclear. Based on amino acid substitution studies for those residues that provide the first shell of non-covalent interactions with FeMo-cofactor we previously targeted a specific 4Fe-4S face of FeMo-cofactor approached by the MoFe protein α-subunit residues α-70^Val and α-96^Arg as providing the substrate binding and reduction site. In the present work, support for this hypothesis was obtained by showing that substitution of the α-70^Val residue by α-70^Ala relaxes constraints within the substrate-binding pocket so that effective reduction of the short chain alkynes, propargyl alcohol and propyne, which are not effectively reduced by the wild type enzyme, is now permitted.

Introduction

Nitrogenase is a two-component metalloenzyme that catalyzes the MgATP-dependent reduction of N_2. It is also able to reduce a variety of other multiply bonded substrates, the most familiar one being acetylene, which can be reduced by two electrons to yield ethylene.[1,2] In the absence of other substrates, protons are reduced by nitrogenase to yield H_2. During catalysis the 60 kDa Fe protein dimer (component II) delivers electrons to the 250 kDa $\alpha_2\beta_2$ MoFe protein (component I) which provides the substrate reduction site. Initial intercomponent electron transfer is thought to proceed from the solvent exposed [4Fe-4S] cluster of the Fe protein to an [8Fe-7S] cluster located within the MoFe protein, called the P-cluster, one of which is located between each αβ-subunit pair. Electrons are subsequently delivered from the P-cluster to the substrate-binding site provided by a [7Fe-9S-Mo-Homocitrate] cluster called FeMo-cofactor (see Christiansen *et al.*[3] for a recent review). One FeMo-cofactor is contained within each MoFe protein α-subunit and each MoFe protein αβ unit is considered to comprise an individual catalytic entity. FeMo-cofactor is constructed from [4Fe-3S] and [3Fe-3S-Mo] subfragments joined by three bridging sulfides with homocitrate attached to the Mo atom through its 2-hydroxy and 2-carboxyl groups, Fig. 1.[4–6]

How do substrates interact with and become activated at the metal–sulfur surface of FeMo-cofactor? This question has proven difficult to answer for several reasons. First, although intact FeMo-cofactor can be separated from purified MoFe protein,[7] FeMo-cofactor removed from its polypeptide matrix does not effectively reduce any substrate. Second, no significant substrate interaction with FeMo-cofactor has been detected for the MoFe protein in its as-isolated resting state. Rather, productive substrate interaction, which can be detected in

certain cases by EPR spectroscopy, see Fisher *et al.*[8] for a recent example, only occurs at redox levels of the enzyme below the resting state, and this requires the addition of Fe protein and MgATP under turnover conditions. Although spectroscopic analysis of nitrogenase under catalytic conditions has proven useful in the formulation of a kinetic description of nitrogenase,[9–12] this approach has provided no mechanistic details about where or how substrates interact with FeMo-cofactor. Finally, because substrates only interact transiently with FeMo-cofactor, and at a redox level below the resting state, crystallographic analysis of the enzyme complex in a substrate-bound form has proven so far to be intractable. Because of these inherent difficulties, formulation of plausible modes for substrate interaction with the metal–sulfur surface of FeMo-cofactor has been confined to theoretical calculations and geometrical considerations. A brief but by no means complete summary of a few of these models is described below.

Deng and Hoffmann used extended Hückel calculations to identify a variety of possible N_2 binding sites on FeMo-cofactor. Three of the models showed N_2 replacing one of the bridging S ligands within FeMo-cofactor, three involved N_2 binding to a 4Fe-4S face, one modeled N_2 in the center of the trigonal six-iron prism and the last modeled the replacement of a terminal Mo-ligand with end-on N_2 binding. These investigators favored a model where N_2 interacts with two adjacent iron atoms of the cluster.[13] Dance used density function calculations based on a symmetric [8Fe-9S] cluster model that is geometrically analogous to the FeMo-cofactor metal–sulfur core. He proposed that the under-coordinated Fe atoms at a 4Fe-4S face of FeMo-cofactor are likely to play an important role in substrate binding whereas adjacent sulfur atoms are involved in proton transfer. The model he favored involves N_2 binding at a single Fe atom.[14,15] Sellmann *et al.* proposed a model where a structural rearrangement of FeMo-cofactor occurs so that a particular face of FeMo-cofactor accommodates substrate binding and activation. This model suggests that a two-electron reduction of FeMo-cofactor occurs prior to N_2 binding at which time a Fe–S–Fe bridge from the intact cluster dissociates and instead ligates with nearby N or O donors from the
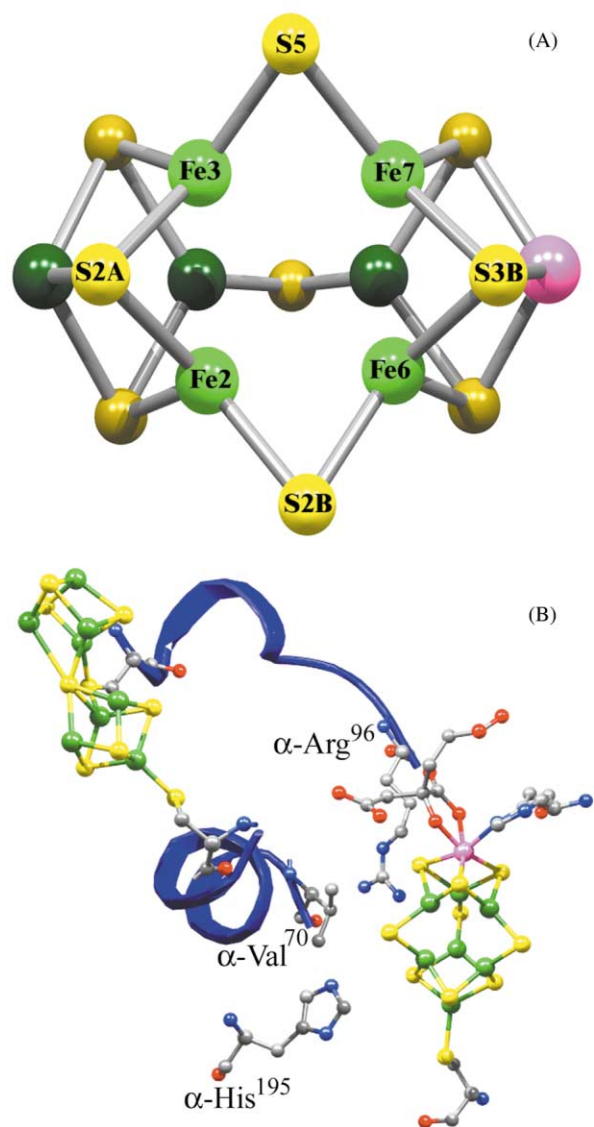
DOI: 10.1039/b107336b

Fig. 1 (A) The FeMo-cofactor metal center excluding the protein ligands and homocitrate. The specific 4Fe-4S face we are targeting is labeled according to the deposited Av1 coordinates in the Protein Data Bank (3MIN) and colored as follows: Fe atoms = bright green, S atoms = bright yellow. The rest of the metal center is colored as follows: Fe atoms = dark green, S atoms = dark yellow, Mo = magenta. (B) Structural organization of the FeMo-cofactor and its polypeptide environment in relationship to the P-cluster. The helices connecting the P-cluster to α-70[Val] and α-96[Arg] are shown as blue ribbons and the α-70[Val], α-96[Arg] and α-195[His] residues capping the specific 4Fe-4S face that is being targeted are labeled. Atom colors are as follows: Mo = magenta, Fe = green, S = yellow, C = grey, O = red and N = blue spheres). Figures produced by Swiss-PDBViewer v3.7b2.[43]

polypeptide environment. N_2 subsequently binds in a bridging mode between the two 'open' Fe atoms. In this model the role of the Mo atom in catalysis is suggested to involve fine-tuning the redox potential of the cluster.[16,17] Szilagyi *et al.* targeted the Mo-site and its ligand environment using a hybrid density function method (B3LYP). In line with a model previously proposed by Grönberg *et al.*[18] they suggested rearrangement of the homocitrate from bidentate to monodentate coordination as a way to accommodate N_2 binding at the Mo atom.[19]

As an alternative but complementary strategy to these theoretical approaches we have taken a direct experimental approach for identification of the substrate interaction site by manipulating the polypeptide environment of FeMo-cofactor using amino acid substitution. Towards this end we recently described a genetic selection which resulted in the production of an altered nitrogenase MoFe protein from *Azotobacter vinelandii* that is able to effectively reduce N_2 but is significantly

impaired in its ability to reduce acetylene.[20] Based on the location and nature of the substituting residue that gives rise to this phenotype (MoFe protein α-69[Gly] residue substituted by α-69[Ser]), we proposed that the 4Fe-4S face of FeMo-cofactor capped by α-70[Val] and α-96[Arg] within the MoFe protein provides the substrate binding site (Fig. 1).[20,21] Namely, we suggested that the α-69[Ser] substitution has an indirect effect on acetylene binding within the altered protein by impacting the dynamic movement of the side-chains of either or both α-70[Val] and α-96[Arg] during catalysis. As a way to test this hypothesis and to determine if it is possible to relax the substrate selectivity of nitrogenase, we substituted the α-70[Val] residue within the MoFe protein by α-70[Ala] and determined the physiological and catalytic consequences of this substitution.

Results

Substitution of the MoFe protein α-70[Val] residue by α-70[Ala] results in physiogical sensitivity to propargyl alcohol

A mutant *A. vinelandii* strain having the α-70[Val] residue substituted by α-70[Ala] was constructed using site-directed mutagenesis and gene replacement techniques. The strain producing the α-70[Ala]-substituted MoFe protein (designated DJ1310) was capable of normal diazotrophic growth and was therefore not compromised in its ability to reduce N_2. To determine if constraints on substrate interaction were relaxed for the α-70[Ala] MoFe protein, the effect of adding propargyl alcohol (propargyl-OH) to the growth medium under nitrogen-fixing conditions was evaluated for DJ1310 and the parental wild type strain (Fig. 2). Propargyl-OH was chosen for this analysis
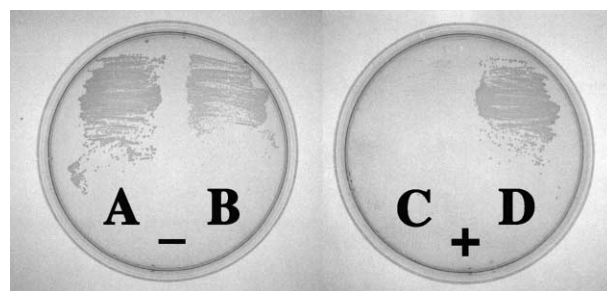

Fig. 2 Effect of propargyl-OH on diazotrophic growth of wild type *A. vinelandii* and strain DJ1310. Strain DJ1310 produces an altered MoFe protein having the α-70[Val] residue substituted by α-70[Ala]. Cells are spread on minimal medium petri plates having no added source of fixed nitrogen. The petri plate on the left has strain DJ1310 (A) and wild type (B) spread on minimal medium containing no fixed nitrogen source and no added propargyl-OH. The petri plate on the right has strain DJ1310 (C) and wild type (D) spread on minimal medium containing no fixed nitrogen source with 6 mM propargyl-OH added. Photographs of the petri plates were taken after one week of growth. Notice there is no diazotrophic growth of strain DJ1310 in the presence of 6 mM propargyl-OH (C).

because it is a relatively small substituted-acetylene molecule that is also a water-soluble liquid at ambient temperature. The addition of 6 mM propargyl-OH to the growth medium completely inhibited diazotrophic growth of strain DJ1310 but had little or no effect on diazotrophic growth of the wild type strain. The addition of 6 mM propargyl-OH had no effect on the growth of either strain when a source of fixed nitrogen was also added to the growth medium, indicating that the effect is specific for physiological N_2 fixation.

Propargyl-OH inhibition of proton reduction, N_2 reduction and acetylene reduction catalyzed by the α-70[Ala] MoFe protein

To determine the basis for propargyl-OH inhibition of diazotrophic growth by DJ1310, the substituted MoFe protein from this strain was purified and the effect of propargyl-OH on the reduction of other substrates examined. It is known that for

nitrogenase catalysis a mixture of different substrates will compete with each other for the available reducing equivalents without affecting the overall rate of electron flux. Thus, the interaction of propargyl-OH with the α-70^{Ala} MoFe protein was first evaluated by its ability to inhibit either proton reduction or N_2 reduction. These analyses (Fig. 3) show that propargyl-OH is
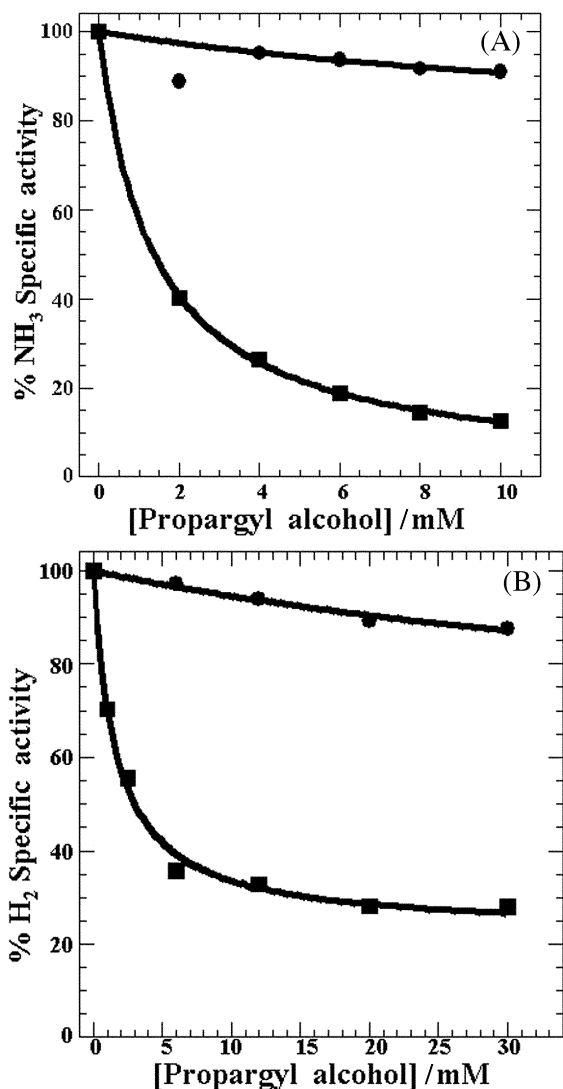

Fig. 4 Lineweaver–Burk plot showing competitive inhibition by propargyl-OH on acetylene reduction catalyzed by the α-70^{Ala} MoFe protein. No addition (solid circles), plus 1.5 mM propargyl-OH (squares), plus 3.0 mM propargyl-OH (triangles), plus 5.0 mM propargyl-OH (open circles). V_{max} corresponds to 1600 nmol acetylene formed per min per mg MoFe protein.

To distinguish whether or not propargyl-OH is only a flux inhibitor (*i.e.* inhibitor of electron flow), or also a substrate that competes with other substrates for available reducing equivalents, we assayed for a product of propargyl-OH reduction catalyzed by the α-70^{Ala} MoFe protein. Gas chromatographic analysis of the reaction vial headspace after incubation of propargyl-OH with the α-70^{Ala} MoFe protein under catalytic conditions did not reveal the time-dependent accumulation of any detectable propyne or allene, potential products of the two-electron reduction of propargyl-OH. However, very small amounts of the four-electron reduction product, propene, could be detected. Nevertheless, the formation of propene occurred at a rate of less than 5 nmol product per min per mg MoFe protein, far below levels that could account for the propargyl-OH inhibition of proton or N_2 reduction catalyzed by the α-70^{Ala} MoFe protein.

The other remaining possible product from the two-electron reduction of propargyl-OH is allyl alcohol (allyl-OH). As described in the Experimental section, a GC-mass spectrometry method was used for identification and quantitation of allyl-OH as a product of α-70^{Ala} MoFe protein catalyzed propargyl-OH reduction. When propargyl-OH was used as substrate for the α-70^{Ala} MoFe protein a significant amount of allyl-OH formation could be detected. Under the conditions used for these experiments a maximum level of 400 nmol min^{-1} of allyl-OH was produced per mg of the α-70^{Ala} MoFe protein. However, because of the inherent difficulties in accurately quantifying allyl-OH, whether or not propargyl-OH is an inhibitor of electron flux, in addition to its ability to serve as a relatively effective substrate, could not be determined with certainty. There was not a sufficient amount of allyl-OH formation catalyzed by the wild type enzyme to permit its detection by GC-mass spectrometry, consistent with the ineffectiveness of propargyl-OH as an inhibitor of the wild type enzyme.

Propyne is an effective substrate for the α-70^{Ala} MoFe protein

Because propargyl-OH proved to be a substrate for the α-70^{Ala} MoFe protein, but not for the wild type protein, we determined if propyne could also be used as a substrate for the α-70^{Ala} MoFe protein. In contrast to allyl-OH formation catalyzed by propargyl-OH reduction, propene, the product of two-electron reduction of propyne, can be easily and accurately determined by gas chromatography. It is already known that propyne is an extremely poor substrate for the wild type enzyme.[22,23] Data

Fig. 3 Propargyl-OH inhibition of NH_3 production (A) and H_2 production (B) catalyzed by the wild type (solid circles) and α-70^{Ala}-substituted (solid squares) MoFe proteins. NH_3 formation assays were conducted under 1 atm of N_2 and H_2 production assays were conducted under 1 atm Ar. (N.B. 100% activity for wild type NH_3 and H_2 production were 1900 and 2300 nmol product per min per mg MoFe protein, respectively. 100% activity for the α-70^{Ala}-substituted MoFe protein maximum for NH_3 and H_2 production were 800 and 1800 nmol product per min per mg MoFe protein, respectively).

a potent inhibitor of both proton and N_2 reduction catalyzed by the α-70^{Ala} MoFe protein. In each case, 2 mM propargyl-OH resulted in approximately 50% inhibition. In contrast, propargyl-OH is only a very poor inhibitor of the reduction of the same substrates by the wild type MoFe protein. To evaluate the capacity for propargyl-OH to inhibit acetylene reduction catalyzed by the α-70^{Ala} MoFe protein, a series of substrate saturation curves were obtained using acetylene as the substrate and increasing concentrations of propargyl-OH as the inhibitor. The results of these measurements (Fig. 4) show that, for the α-70^{Ala} MoFe protein, propargyl-OH is a reversible, competitive inhibitor of acetylene reduction having a K_i of approximately 4.0 mM. In contrast, propargyl-OH is such a poor inhibitor of acetylene reduction catalyzed by the wild type enzyme that a K_i could not be accurately calculated.
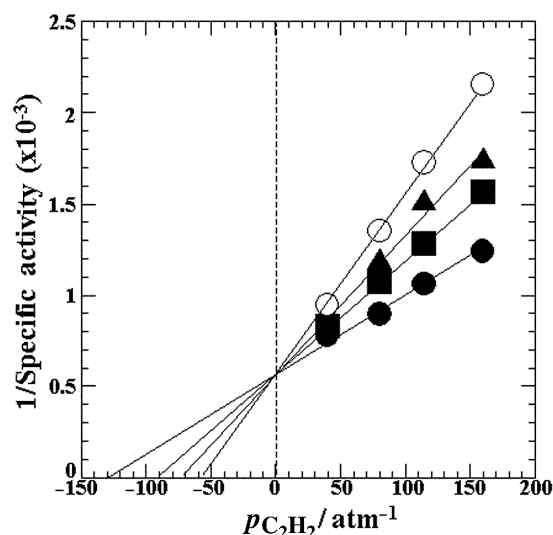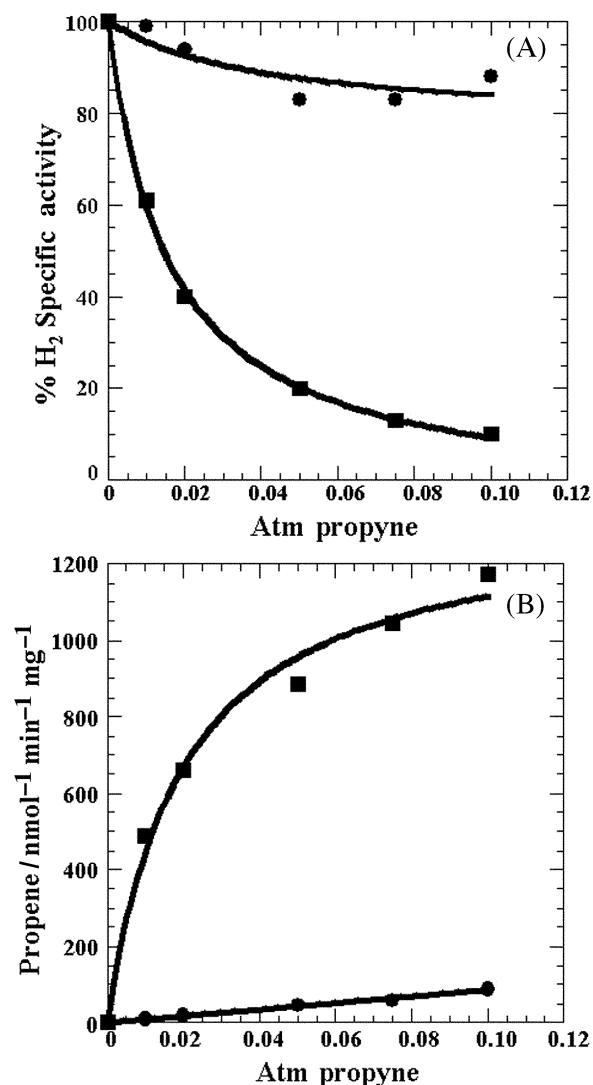
Fig. 5 Propyne inhibition of H_2 production (A) and reduction of propyne to yield propene (B) catalyzed by the wild type (circles) and α-70^Ala-substituted MoFe protein (squares). 100% H_2 production is 2300 nmol per min per mg MoFe for wild type and 1800 nmol per min per mg for the α-70^Ala substituted MoFe protein. A Michaelis–Menten kinetic fit for the reduction of propyne by the α-70^Ala-MoFe protein gives K_m and V_{max} values of 0.02 atm propyne and 1350 nmol propene produced per min per mg MoFe protein, respectively.

shown in Fig. 5 reveal that propyne is an effective inhibitor of proton reduction catalyzed by the α-70^Ala MoFe protein, as well as an effective substrate for that enzyme. The product of propyne reduction catalyzed by the α-70^Ala MoFe protein was found to be propene on the basis of its gas chromatographic retention time when compared to a propene standard. Data shown in Fig. 5 also confirm that propyne is only a very poor substrate for the wild type MoFe protein. In the case of propyne reduction catalyzed by the α-70^Ala MoFe protein, propane, the four-electron reduction product, could not be detected. It was also found that, like the wild type MoFe protein, the α-70^Ala MoFe protein does not catalyze the four-electron reduction of acetylene to yield ethane.

Discussion

An approach frequently used to identify active sites in enzymes involves using genetic selection for strains resistant to the physiological effects of substrate analogs. We previously used this approach to isolate a mutant strain of *A. vinelandii* that is resistant to the short chain alkyne acetylene.[20] Acetylene is an effective nitrogenase substrate[1,2] and a potent inhibitor of physiological N_2 reduction.[1,24,25] Nitrogenase isolated from an

A. vinelandii acetylene-resistant strain is not significantly affected in its ability to reduce N_2 but is severely impaired in its ability to reduce acetylene. The altered MoFe protein from this strain was shown to have the α-subunit 69^Gly residue substituted by α-69^Ser.[20] Within the wild type enzyme the α-69^Gly residue is located immediately adjacent to the α-70^Val residue, whose side-chain approaches one of the three geometrically identical 4Fe-4S faces of FeMo-cofactor [4-6] (Fig. 1). Another residue, α-96^Arg also approaches the same 4Fe-4S face of FeMo-cofactor and potentially interacts with the α-69^Gly residue through hydrogen bonding of a nitrogen atom within its guanidino group to the carbonyl oxygen of α-69^Gly (Fig. 1). Based on these observations we proposed that the 4Fe-4S face of FeMo-cofactor approached by α-70^Val and α-96^Arg provides an acetylene-binding site and that the α-69^Ser substitution results in movement of either or both α-70^Val and α-96^Arg so that effective interaction of acetylene with the active site is prevented.

Previous work has shown that, although acetylene is an effective nitrogenase substrate, other alkynes such as propyne are not.[23,26] An explanation offered for this observation is that constraints within the substrate-binding pocket prevent the binding of short chain alkynes larger than acetylene.[26,27] Evidence supporting this view was provided by the observation that, while propyne is only a very poor nitrogenase substrate, cyclopropene is a relatively effective substrate.[23] Thus, if our hypothesis that the 4Fe-4S face approached by α-70^Val provides the substrate-binding site is correct, we reasoned that shortening the aliphatic side-chain of α-70^Val could result in expanding the substrate reduction capability of nitrogenase to include short chain alkynes in addition to acetylene. Results reported here show that substitution of the α-70^Val residue by α-70^Ala does result in an altered MoFe protein that is able to catalyze the effective reduction of propargyl-OH and propyne, neither of which is an effective substrate for the wild type enzyme. These results can be interpreted in light of what is known about nitrogenase catalysis and the crystallographic structure of the MoFe protein.

It is currently believed that during nitrogenase turnover electrons are delivered from the P-cluster to the substrate reduction site provided by FeMo-cofactor. Inspection of the MoFe protein structure shows that a short helix spans the region between the P-cluster and FeMo-cofactor (Fig. 1). This helix originates with α-62^Cys, which provides a thiolate ligand to one P-cluster subfragment, and ends at α-70^Val capping one side of a specific 4Fe-4S face of FeMo-cofactor. Another short helix extends from α-88^Cys, which provides a bridging ligand to both P-cluster subfragments, and ends at α-96^Arg capping the other side of the same 4Fe-4S face of FeMo-cofactor. Thus, of the three geometrically identical 4Fe-4S faces of FeMo-cofactor, this one is in closest proximity to the P-cluster and, therefore, most appropriately positioned for receiving electrons delivered from the P-cluster. Hence, this 4Fe-4S face is an attractive candidate for providing a substrate-binding site. Our data provide support for this possibility because shortening of the aliphatic side-chain of α-70^Val permits the accommodation of larger alkyne substrates not effectively reduced by the wild type enzyme. Although we cannot yet rule out the possibility of indirect structural perturbations at another face of FeMo-cofactor, or an indirect rearrangement in the environment surrounding the Mo atom, we do not favor these possibilities for two reasons. First, structural perturbations within the FeMo-cofactor polypeptide environment are frequently manifested by a significant alteration in the EPR spectrum, yet there are no such alterations in the EPR spectrum in the altered MoFe protein having the α-70^Ala substitution. Second, substitutions that significantly alter the polypeptide environment of FeMo-cofactor would also be expected to have a severe effect on substrate reduction. However, the α-70^Ala substitution expands the ability of the altered MoFe protein to include

propargyl-OH and propyne with only a modest effect on the ability of the enzyme to reduce protons, acetylene or N_2. Based on these considerations we conclude that, for the α-70[Ala] MoFe protein, propargyl-OH and propyne bind at the 4Fe-4S face capped by α-70[Val] and α-96[Arg]. However, this conclusion does not rule out the possibilities that either of the other two 4Fe-4S faces of FeMo-cofactor, or the Mo atom, are able to provide substrate-binding sites under certain conditions. These issues will need to be resolved with other experiments. Nevertheless, our working model is that Mo is not directly involved in providing a substrate-binding site and that most or all nitrogenase substrates are bound and are reduced at the same 4Fe-4S face.

Inspection of the resting-state crystal structure of the MoFe protein indicates that when van der Waals repulsion forces are considered there is very little room for substrates other than protons to have access to the 4Fe-4S face of FeMo-cofactor capped by the α-70[Val] and α-96[Arg] side-chains. In fact, there does not appear to be any way to accommodate a bridging mode for substrates between Fe atoms in the resting state of the enzyme. This binding configuration is often cited as a likely possibility because of the *cis* stereospecificity for proton addition when C_2D_2 is used as substrate.[1,28] Consequently, if our model is correct and substrates do bind at this 4Fe-4S face, then the side-chains of either or both α-70[Val] and α-96[Arg] must move during catalysis to accommodate substrate binding. Close examination of the crystallographic model indicates that it is unlikely the α-70[Val] side-chain would be capable of substantial movement without a significant rearrangement in the polypeptide structure. In contrast, there does appear to be sufficient space to accommodate movement of the α-96[Arg] side-chain. We find this possibility attractive for three reasons. First, movement of the α-96[Arg] is consistent with a possible role for its side-chain as a proton shuttle between the pool of water surrounding homocitrate and the substrate-binding site. Second, comparison of MoFe protein crystal structures from *A. vinelandii*,[4,5] *Clostridium pasteuranium*,[29] *Klebsiella pneumoniae*[6] as well as the *A. vinelandii* ADP·ALF$_4$ stabilized complex[30] reveals this side-chain occupies slightly different positions in each structure, indicating the possibility for their dynamic movement during catalysis. Finally, in other amino acid substitution experiments we found that shortening of the α-96[Arg] side-chain permits the binding of certain substrates to the MoFe protein in the resting state.[31]

In summary, results reported here indicate that short chain alkynes can bind and be reduced at a specific 4Fe-4S face of FeMo-cofactor. These results should be useful for future modeling studies and also provide the basis for other amino acid substitution experiments designed to determine exactly where and how substrates interact with FeMo-cofactor.

Experimental

Strain construction, cell growth, and purification

A mutant strain of *A. vinelandii* having the α-70[Val] residue substituted by α-70[Ala] was constructed using site-directed mutagenesis and gene replacement methods previously described in detail.[32–35] Cells were grown and derepressed for nif gene expression and harvested as described previously.[35] Crude extracts were prepared by the osmotic shock method and purified as previously described.[35] Quantitation of protein was performed by a modified biuret method using bovine serum albumin as the standard[36] and protein purity assessed by SDS-polyacrylamide gel electrophoresis.[37] All protein manipulations were kept anaerobic through the use of a Schlenk apparatus fitted with a BASF catalyst tower.[38]

Kinetic assays

The overall technique and reaction mixture composition are described elsewhere.[39,40] Each assay contained 0.05 mg of MoFe protein and 0.45 mg of Fe protein to give a 36 : 1 molar ratio of Fe protein to MoFe protein. Acetylene was freshly prepared for each experiment by the reaction of calcium carbide and water. Propyne (98% pure) was purchased from Aldrich. A propargyl-OH stock solution was anaerobically prepared by the addition of appropriate amounts of propargyl alcohol and 0.25 M Hepes [*N*-(2-hydroxyethyl)piperazine-*N'*-(2-ethanesulfonic acid)] buffer pH 7.4 to an evacuated crimp sealed vial to give a final concentration of 1 M. Assays were initiated by the addition of Fe protein and the reaction allowed to proceed for 8 min while shaking in a 30 °C water bath and subsequently terminated by the addition of 250 μl of a 0.4 M EDTA solution. H_2 production was monitored by injection of 200 μl of the reactions gas phase into a Shimadzu GC-14 gas chromatograph equipped with a Supelco 80/100 molecular sieve 5A column and a thermal conductivity detector. Ethylene and propene production were monitored using a Hewlett-Packard 5890A gas chromatograph equipped with an Al_2O_3 capillary column and a flame ionization detector.

Inhibition patterns were evaluated by examination of Lineweaver–Burk double reciprocal plots of the kinetic assay data. Michaelis–Menten constants were derived by fitting data to the following hyperbolic equation: $v = ([S]V_{max})/(K_m + [S])$.

Extraction and quantification of propargyl alcohol and allyl alcohol from incubation mixtures

The reaction mixture was quenched by addition of EDTA as described above and the liquid was transferred to a 2 ml glass vial. Analytes were extracted from the solution by submerging an SPME fiber into the solution for 20 min.[41,42] (N.B. A detailed protocol for this method is described in Supelco, Bulletin 901). The fiber was then inserted into a Hewlett-Packard 5790 gas chromatograph that was interfaced to a VG7070E-HF mass spectrometer. The system was operated in the splitless injection mode with a helium head pressure of 12 psi. The gas chromatograph injection port [220 °C], and the purge valve were opened after 0.25 min. The SPME fiber was conditioned for an additional 0.75 min in the hot injection port prior to the next analysis. The column oven temperature was programmed from 45 °C to 120 °C at 5 °C min^{-1}. The mass spectrometer source was operated in the electron impact mode at 70 eV at 200 °C. The magnetic field was scanned from 10 to 200 amu in 0.5 seconds. Allyl-OH and propargyl-OH eluted at 1.22 min and 1.30 min, respectively. Quantification was performed by measuring the area under the chromatographic peak in a mass chromatogram of the base peak in the mass spectrum of each compound (*m/z* 57 for allyl-OH and *m/z* 55 for propargyl-OH). Although the gas chromatographic peaks were not completely resolved, quantification was possible because there was no significant ion intensity for *m/z* 55 in the propargyl-OH alcohol spectrum, nor of *m/z* 57 in the allyl-OH spectrum.

Acknowledgements

References

1 M. J. Dilworth, *Biochim. Biophys. Acta*, 1966, **127**, 285.
2 R. Schöllhorn and R. H. Burris, *Proc. Natl. Acad. Sci. USA*, 1967, **58**, 213.
3 J. Christiansen, D. R. Dean and L. C. Seefeldt, *Annu. Rev. Plant Physiol. Plant Mol. Biol.*, 2001, **52**, 269.
4 J. Kim and D. C. Rees, *Nature*, 1992, **360**, 553.
5 J. W. Peters, M. H. B. Stowell, S. M. Soltis, M. G. Finnegan, M. K. Johnson and D. C. Rees, *Biochemistry*, 1997, **36**, 1181.
6 S. M. Mayer, D. M. Lawson, C. A. Gormal, S. M. Roe and B. E. Smith, *J. Mol. Biol.*, 1999, **292**, 871.
7 V. K. Shah and W. J. Brill, *Proc. Natl. Acad. Sci. USA*, 1977, **74**, 3249.

8 K. Fisher, W. E. Newton and D. J. Lowe, *Biochemistry*, 2001, **40**, 3333.
9 R. N. F. Thorneley and D. J. Lowe, *Biochem. J.*, 1984, **224**, 903.
10 R. N. F. Thorneley and D. J. Lowe, *Biochem. J.*, 1984, **224**, 887.
11 D. J. Lowe and R. N. F. Thorneley, *Biochem. J.*, 1984, **224**, 895.
12 D. J. Lowe and R. N. F. Thorneley, *Biochem. J.*, 1984, **224**, 877.
13 H. B. Deng and R. Hoffmann, *Angew. Chem.*, 1993, **32**, 1062.
14 I. G. Dance, *Aust. J. Chem.*, 1994, **47**, 979.
15 I. G. Dance, *Chem. Commun.*, 1997, **2**, 165.
16 D. Sellmann and J. Sutter, *J. Biol. Inorg. Chem.*, 1996, **1**, 587.
17 D. Sellmann and A. Fursattel, *Coord. Chem. Rev.*, 2000, **200–202**, 545.
18 K. L. C. Gronberg, C. A. Gormal, M. C. Durrant, B. E. Smith and R. A. Henderson, *J. Am. Chem. Soc.*, 1998, **120**, 10613.
19 R. K. Szilagyi, D. G. Musaev and K. Morokuma, *Inorg. Chem.*, 2001, **40**, 766.
20 J. Christiansen, V. L. Cash, L. C. Seefeldt and D. R. Dean, *J. Biol. Chem.*, 2000, **275**, 11459.
21 J. Christiansen, L. C. Seefeldt and D. R. Dean, *J. Biol. Chem.*, 2000, **275**, 36104.
22 R. W. F. Hardy and E. K. Jackson, *Fed. Proc.*, 1967, **26**, 725.
23 C. E. McKenna, M.-C. McKenna and C. W. Huang, *Proc. Natl. Acad. Sci. USA.*, 1979, **76**, 4773.
24 J. C. Hwang, C. H. Chen and H. Burris, *Biochim. Biophys. Acta*, 1973, **29**, 256.
25 J. M. Rivera-Ortiz and R. H. Burris, *J. Bacteriol.*, 1975, **123**, 537.
26 C. E. McKenna, in *Molybdenum and Molybdenum Containing Enzymes*, ed., M. Coughlan, Pergamon Press, New York, 1980.
27 R. C. Burns and R. W. F. Hardy, in *Molecular Biology, Biochemistry and Biophysics Series*, ed., A. Kleinzeller, G. F. Springer and H. G. Wittman, Springer-Verlag, New York, 1975, vol. 21.
28 R. W. F. Hardy, R. D. Holsten, E. K. Jackson and R. C. Burns, *Plant Physiol.*, 1968, **43**, 1185.
29 J. T. Bolin, N. Campobasso, S. W. Muchmore, T. V. Morgan and L. E. Mortenson, in *Molybdenum enzymes, cofactors and model systems*, ed., E. I. Stiefel, D. Coucouvanis and W. E. Newton, American Chemical Society, Washington, DC, 1993, pp. 186–195.
30 H. Schindelin, C. Kisker, J. L. Sehlessman, J. B. Howard and D. C. Rees, *Nature*, 1997, **387**, 370.
31 P. M. C. Benton, S. M. Mayer, J. Shao, B. M. Hoffman, D. R. Dean and L. C. Seefeldt, *Biochemistry*, 2001, in press.
32 W. J. Page and M. von Tigerstrom, *J. Bacteriol.*, 1979, **139**, 1058.
33 A. C. Robinson, B. K. Burgess and D. R. Dean, *J. Bacteriol.*, 1986, **166**, 180.
34 M. R. Jacobson, V. L. Cash, M. C. Weiss, N. F. Laird, W. E. Newton and D. R. Dean, *Mol. Gen. Genet.*, 1989, **219**, 49.
35 J. Christiansen, P. J. Goodwin, W. N. Lanzilotta, L. C. Seefeldt and D. R. Dean, *Biochemistry*, 1998, **37**, 12611.
36 V. Chromy, J. Fischer and V. Kulhanek, *Clin. Chem.*, 1974, **20**, 1362.
37 U. K. Laemmlli, *Nature*, 1970, **227**, 680.
38 B. K. Burgess, D. B. Jacobs and E. I. Stiefel, *Biochem. Biophys. Acta*, 1980, **614**, 196.
39 J. W. Peters, K. Fisher and D. R. Dean, *J. Biol. Chem.*, 1994, **269**, 28076.
40 C. H. Kim, W. E. Newton and D. R. Dean, *Biochemistry*, 1995, **34**, 2798.
41 Supelco, Inc., Bulletin, Sigma-Aldrich Co., 1997, 901, 65.
42 D. A. Cassada, Y. Zhang, D. D. Snow and R. F. Spalding, *Anal. Chem.*, 2000, **72**, 4654.
43 N. Geux and M. C. Peitsch, *Electrophoresis*, 1997, **18**, 2714.